

# Numerical Simulation of the Thermal Convection and Subduction Process in the Mantle

Project Representative

Yoshio Fukao      Institute for Research on Earth Evolution, Japan Agency for Marine-Earth Science and Technology

Authors

Yoshio Fukao<sup>\*1</sup>, Masanori Kameyama<sup>\*2</sup>, Takatoshi Yanagisawa<sup>\*1</sup>,  
Yasuko Yamagishi<sup>\*1</sup> and Tomoeaki Nakakuki<sup>\*3</sup>

\*1 Institute for Research on Earth Evolution, Japan Agency for Marine-Earth Science and Technology

\*2 Geodynamics Research Center, Ehime University

\*3 Department of Earth and Planetary Systems Science, Hiroshima University

The aim of this project is to make up a comprehensive model of the dynamics and evolution of the Earth's mantle, and to simulate phenomena related with subduction. (1) With the regional modeling focusing on subduction process, we extended our model to three-dimensional one so that it can treat the arbitrary direction of subduction and age difference of the plate. The three-dimensional model confirmed that both viscosity jump in the lower mantle and the trench retreat are essential for the stagnation of slabs, that is consistent with two-dimensional modelings, and it succeeded in reproducing the varying behavior of subducting plate along a trench. (2) With the global modeling in Earth-like spherical shell geometry, we made systematic research on the patterns and heat transport for the wide range of Rayleigh numbers. The typical wavelength of convection pattern gets shorter for higher Rayleigh number, and the patterns for  $Ra > 10^8$  are characterized by the vertical motions of numerous small plumes. We conclude that the amount of heat flow, Nusselt number, depends on about 0.31 power of Rayleigh number.

**Keywords:** mantle convection, subducting slab, convective heat transport

## 1. Introduction

The Earth's mantle is composed of solid rocks but it flows like a viscous fluid in a geologic time scale. This convective flow of the mantle is emerging as the motion of tectonic plates on the Earth's surface. The motion of surface plates causes earthquake, volcanism and mountain building at the plate margins. And as the mantle flow transports the heat from the hot interior, the whole of the Earth has been cooling through its history. Hence, mantle convection is the key process for understanding the activity and evolution of our planet.

We can see the internal structure of the Earth's mantle by seismic tomography. It illustrates the behavior of slabs, that is, subducted plates in the mantle. Some of the slabs stagnate in the mantle transition zone while the others penetrate into the lower mantle. Because slabs are the downwelling portions of the mantle convection, the mechanisms to generate the various styles of subducted slabs in the mantle transition zone are important to understand the structure and dynamics of the mantle. We have been studying the process of stagnation and penetration of slabs, and succeeded in simulating both behaviors and clarifying the conditions for slab stagnation in FY2006 by using two-dimensional regional model.

Our two-dimensional model can reproduce the general behavior of slabs under natural setting, but it has limitations in applying for specific subduction zones of the Earth. Three-dimensional structure is essential for some subduction zones especially located in western Pacific region. Figure 1 is the structure of the mantle relating to the subduction of Pacific plate from global tomography [1]. These two cross sections belong to one series of subduction zone, but the styles are very different; around Mariana, the slab is penetrating to the lower mantle; around Japan, it is stagnating at the transition zone. In FY 2007, we extended our regional model for treating such kind of three-dimensionality (Section 2).

With the regional modeling we focus on the behavior of subducting slabs whose time scale is less than hundred million years, on the other hand, the global modeling in Earth-like spherical shell geometry for longer time scale is also our target. Global modeling with spherical shell is indispensable for the understanding of the convection pattern and heat transport of the mantle through its history. We have been developing the numerical code for thermal convection in spherical shell, and we achieved the Rayleigh number up to  $10^9$  that can

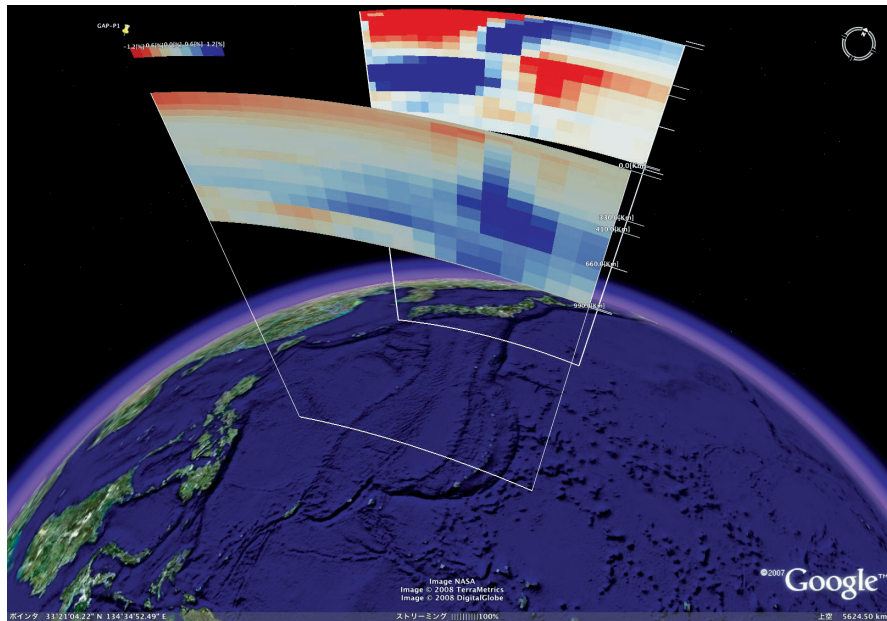


Fig. 1 Two cross sections of seismic tomography for subduction of Pacific plate (drawn by the dataset GAP-P1 [1]). The P-wave velocity anomalies are shown from surface to 1000 km depth, and the color scale is  $\pm 1.2\%$ . Indicated in blue are the regions of fast anomalies, while in red are those of slow anomalies. The Pacific Plate is subducting under the Philippine Sea Plate at both of these cross sections, but the image of subducted slab is very different. You can draw arbitrary vertical cross sections at "<http://www.jamstec.go.jp/pacific21/TMGonGE/home.html>".

cover most of the history of the mantle. We report on the basic features of thermal convection in spherical shell with their Rayleigh number dependences in Section 3.

## 2. Regional model: Three-Dimensional Numerical Simulations on Dynamic Behaviors of Subducting Slabs

We are developing numerical models of mantle convection in order to study the effects of three-dimensionality on the formation and the dynamic behaviors of stagnant slabs. A time-dependent thermal convection of Boussinesq fluid in a three-dimensional rectangular box of 1320 km height and aspect ratio of  $6 \times 6 \times 1$  is considered. We have included both the exothermic olivine to spinel and the endothermic spinel to perovskite phase transitions at around 410 and 660 km depths from the top surface, respectively. The viscosity of mantle material is assumed to be exponentially dependent on temperature. We also take into account the effects of the sudden increase in viscosity at the 660 km depth. The distribution of temperature is initially set by a half-space cooling model moving at a uniform velocity. The cold thermal boundary layer along the top surface is then divided into two sections, by introducing a "plate boundary" (or a "trench axis") running in the direction roughly perpendicular to the surface motion. The plate subduction is imposed by applying different kinematic boundary conditions to the upstream and downstream sides of the plate boundary. The motion of the "oceanic" plate on the upstream side is driven by a fixed

velocity at the top surface, while zero motion is set on the surface of the "continental" plate on the downstream side. We also included the effect of maximum yield strength in order to accommodate a strong shear deformation near the plate boundary along the top cold surface. In addition, we take into account the effect of trench migration, by assuming that the computational domain is in relative motion to the stationary mantle. Spatial mesh divisions of up to  $384 \times 384$  in horizontal and 128 in vertical directions are utilized, by the help of the multigrid-based numerical code ACuTEMan [2, 3] designed for large-scale three-dimensional experiments.

We show in Fig. 2 the snapshots taken from several preliminary calculations with different values of the viscosity jump at 660 km depth. In these calculations, the "oceanic" plates on the left-hand side of the top surfaces are assumed to continuously move rightward at a rate of 4.7 cm/year. We also imposed a three-dimensionality of subduction by artificially employing a curvature of the plate boundaries, which yields an along-axis variation of the age of subducting oceanic plates. In the present cases, the ages of subducting plates are set to be 62 Ma and 104 Ma on the near and far vertical side walls, respectively. These differences result in an along-axis variation of the descending velocity of cold slabs. Indeed, the descending velocity is slightly faster at the far sides than at the near sides, despite of uniform plate velocity imposed at the top surface.

The comparison of the cases presented in Fig. 2 clearly indicates that the viscosity jump at 660 km depth tends to

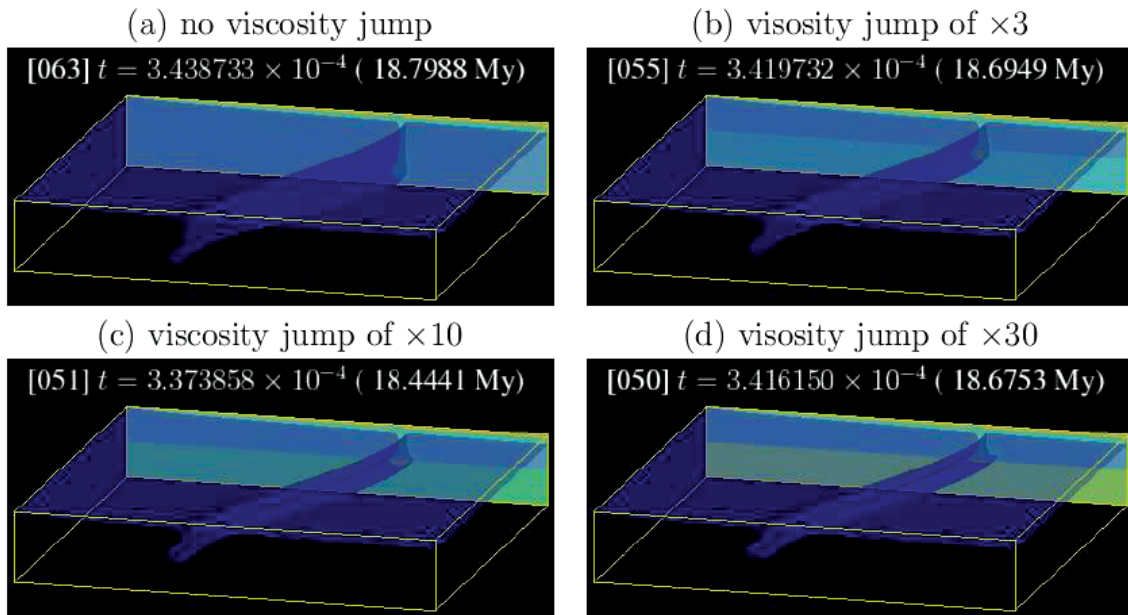


Fig. 2 Snapshots of behaviors of cold subducting plates obtained by time-dependent calculations with different amplitudes of the viscosity jumps at the 660 km depth indicated in the figure. Shown by blue transparent surfaces are the isosurfaces of nondimensional temperature  $T = 0.9$  as a proxy of the bottom surface of oceanic plates. Also shown in color are the distribution of viscosity at the vertical side walls.

barrier the descending motion of subducting slabs across the depth. In the absence of the viscosity jump (Fig. 2a), the tip of the cold slab descends across the phase boundary at 660 km depth, and almost reaches to the bottom surface of the computational domain (1320 km depth). However, with increasing the viscosity jump, the tips of the subducting slabs are stagnated more strongly at the depth of viscosity jumps (Fig. 2b to 2d). These results are in accordance with the recent conjecture that the stagnant slabs are hardly formed solely from the effects of the post-spinel phase transition at around 660 km depth. From these preliminary results we speculate that the further improvement of our numerical models is one promising approach to the reproduction of the stagnant slabs observed on the Earth by, for example, incorporating the effects of the trench retreat. The formations and/or the three-dimensional behaviors of subducting slabs will be discussed in the next FY by systematically studying the effects of various mechanisms, such as phase changes, viscosity stratification, trench retreat, subduction velocity and their along-axis variations.

### 3. Global model: The Natural Pattern of Thermal Convection and its Heat Transport in Spherical Shell Geometry

Simulating thermal convections with simple setting is also important for the understanding of the Earth's mantle convection. Here we focus on the intrinsic patterns of thermal convection and amount of heat transport in spherical shell geometry. The convection pattern is closely related to the size of the structures existing in the mantle. The amount of

heat transport is the key for the activity of whole Earth system and it also regulates the lifetime of the Earth, because planetary evolution is basically the cooling process of the mantle and core. We succeeded in attaining the Rayleigh numbers ( $Ra$ ) over  $10^9$ , which is more than six orders above the critical value. The  $Ra$  of the former numerical studies with highly viscous fluid in Earth-like spherical shell are from critical to around  $10^6$  [4, 5], and up to  $10^8$  by the Earth Simulator [6]. The  $Ra$  of the present Earth's mantle is estimated to be around  $10^7$ , and it has been decreasing through the Earth's history because of the decrease of the heat sources. The  $Ra$  of  $10^9$  that we attained is sufficient to cover most of the history of Earth's mantle convection. Moreover, now we have the complete dataset for the convective motions with  $Ra$  ranging six orders of magnitude, those are quite valuable for establishing the  $Ra$  dependence of the convective heat transport. This is important for the general physics of thermal convection. We made systematic research on the patterns and heat transport with the increase of  $Ra$  under Bousinesq approximation. The  $Ra$  is defined by purely basal heating, and the viscosity of the fluid is constant. The Prandtl number ( $Pr$ ) is set to be infinite, so the inertia term is neglected in the calculation. We use finite element method, and the finest resolution in our simulations is about 15 km at the surface and 256 vertical layers through the mantle. The initial perturbations have small wavelength, and the wavelength of the convection pattern gets longer with the progress of computations then settles in a typical value. We spent enough time steps for each run to get reliable data on the statistically steady state.

It is well known that the convection pattern depends on the  $Ra$ . With the increase of  $Ra$ , the wavelength of convection pattern becomes smaller and the pattern shows unsteady or fluctuating behavior. For the lower  $Ra$ , the convective cells have almost uniform size, but for the higher  $Ra$ , the cells become irregular. All of the convective patterns we simulated have the characteristics as follows; the sheet-shaped downwelling and upwelling flows are generated around the top and the bottom boundaries respectively and they concentrate gradually into cylindrical flows in the convective core region. Figure 3 is the snapshot of the temperature for  $Ra \sim 10^9$ , that is the maximum  $Ra$  in our simulations. Scaling this result to the Earth's mantle, the typical surface flow velocity is 30 cm/year, and the total surface heat flow is 150 TW. Very fine scale plumes go up and down at the mid-

dle depth of the convective layer, and convection 'cell' structures do not exist except for the vicinity to the top and bottom boundaries. These features are seen for  $Ra > 10^8$ .

The  $Ra$  dependences of some statistical values are shown hereafter. Figure 4a is the depth profile of the horizontally averaged temperature for each value of  $Ra$ . These profiles have common features; thermal boundary layers near the top and bottom (with steep temperature gradient where the heat is transported mainly by conduction), and isothermal convective core between them (with little temperature gradient where the heat is transported mainly by the vertical motion of the fluid). The thickness of the thermal boundary layer becomes thinner for higher  $Ra$ . The temperature of the isothermal core ( $\sim 800$  K) is not the center of the top and bottom temperature but close to that of the surface because

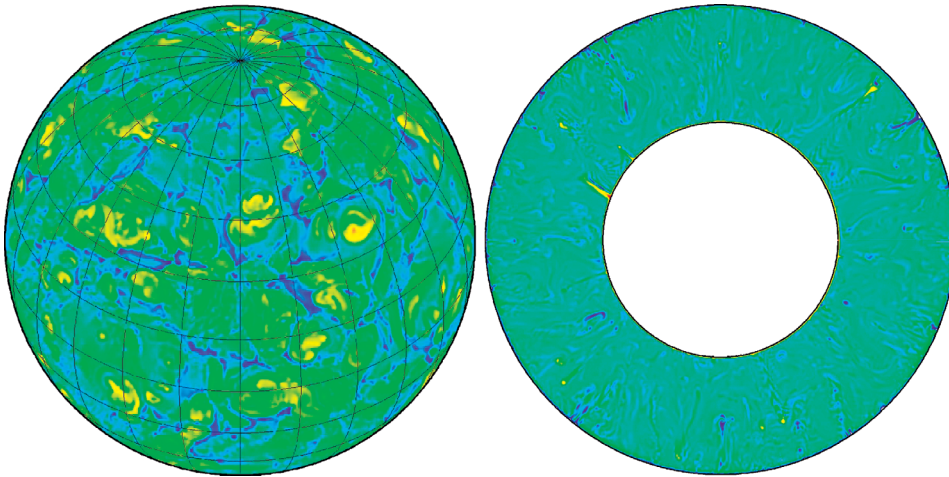


Fig. 3 A snapshot of the convection in spherical shell with  $Ra = 2 \times 10^9$ . Left; temperature just below the surface. Right; temperature cross-section along a meridian. Thin boundary layers exist at the top and bottom, and many small-size plumes are going up and down at the middle depth.

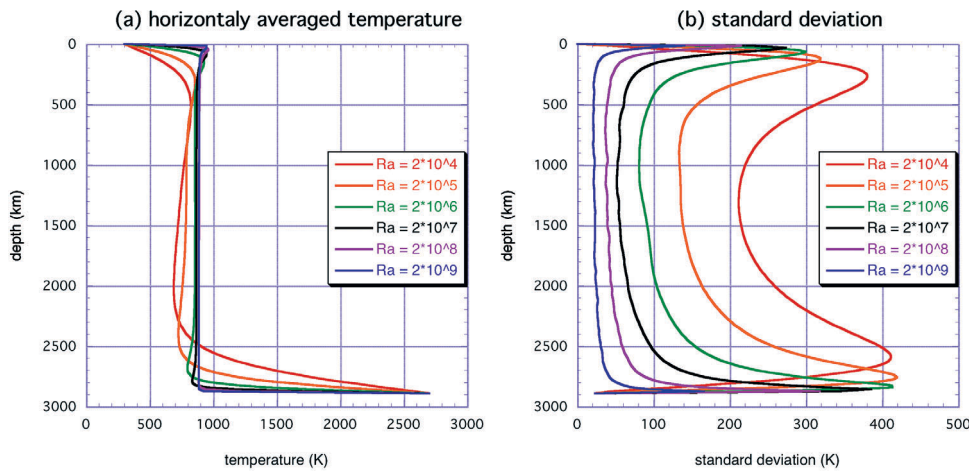


Fig. 4 (a) Horizontally averaged temperature at each depth and its dependence on  $Ra$ . There exist thermal boundary layers at the top and bottom, and isothermal core region between them. The thickness of the thermal boundary layer decreases systematically with the increase of  $Ra$ . (b) Standard deviation of temperature at each depth and its dependence on  $Ra$ . It has large value around the average depth of thermal boundary layer, and smaller value for isothermal core. The deviation for isothermal core region decreases with the increase of  $Ra$ .



of the effect of spherical shell geometry. Figure 4b shows the depth profile of the standard deviation calculated by the horizontal distribution of temperature. This value reflects the range of existing temperature anomaly at each depth. The temperature of the top and bottom boundaries are fixed in our simulations, so the deviation is zero both at the top and bottom. The maximum value of standard deviation is seen around the average depth of the thermal boundary layer, because the thickness of the thermal boundary layer varies horizontally and heterogeneity is large at this depth. Because of the effect of spherical shell geometry, the maximum deviation value is larger for the bottom boundary layer. The standard deviation has smaller value in the isothermal core. With the increase of  $Ra$ , we can see the drastic decrease of the deviation especially for the isothermal core region. This means that at higher  $Ra$  the convective flow is driven by very small horizontal temperature difference inside of the isothermal core region (ex.  $\sim 20$  K for  $Ra \sim 10^9$ ).

The Nusselt number ( $Nu$ ) is defined by the ratio of the total heat transport to the conductive one through the layer. When convection occurs, heat is transported by both fluid motion and conduction, then  $Nu$  becomes more than one.  $Nu$  is the most important value for evaluating the total activity of thermal convections. Therefore, to establish the dependence of  $Nu$  on  $Ra$  is one of the most fundamental problems of thermal convection, and many studies were made both by laboratory and numerical experiments. The  $Ra$ - $Nu$  relationship is known to be dependent on both the wavelength of the convection pattern and the Prandtl number of the fluid.  $Nu$  is thought to be proportional to  $Ra^{1/3}$  for viscous (high  $Pr$ ) fluid with box geometry. Here we can establish the relationship for infinite  $Pr$  fluid with spherical shell. The relationship  $Nu \sim Ra^{0.31}$  is our conclusion, that is quite similar to that of the box geometry. Figure 5 is the summary of  $Ra$ - $Nu$  with spherical shell. Our simulations by using the Earth Simulator extended the range of data drastically. The result of  $Nu$  by our simulations is almost same as the others for smaller  $Ra$ , but they show some discrepancy for  $Ra > 10^5$ ; our  $Nu$  are larger than the result of former studies. In the studies by Ratcliff et al. [4] and Iwase [5], they concluded that  $Nu$  is proportional to  $Ra^{1/4}$ , and they noted that this should be the characteristic of the spherical shell geometry. But they set the initial perturbations as long wavelength ones such as tetrahedral or cubic, and these basic patterns did not change through the time integrations. We can conclude that their weaker dependence of  $Nu$  on  $Ra$  is due to the longer wavelength structure of the convection pattern, and the natural or spontaneous convection patterns for  $Ra > 10^5$  have shorter wavelength for spherical shell geometry. Cubic pattern for  $Ra \sim 10^5$  might be a quasi-steady one, and it takes long time for developing shorter wavelength structure. We propose

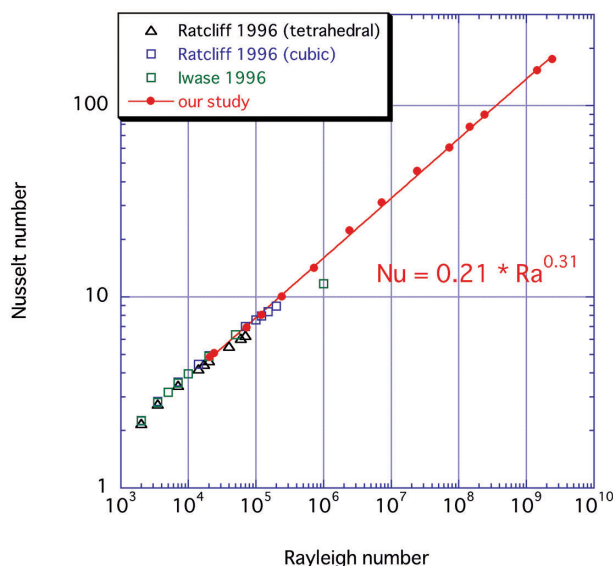


Fig. 5 Summary of the relationship between  $Ra$  and  $Nu$  for spherical shell with infinite  $Pr$  fluid. Our data (red points) suggests  $Nu \sim Ra^{0.31}$  for wide range of  $Ra$ .

that  $Nu \sim Ra^{1/3}$  is also applicable to spherical shell geometry. This means that the ancient Earth's mantle should transport much heat estimated from widely used  $Nu \sim Ra^{1/4}$  relationship, and should cool down in a very short time scale.

## References

- [1] M. Obayashi, H. Sugioka, J. Yoshimitsu, and Y. Fukao, "High temperature anomalies oceanward of subducting slabs at the 410-km discontinuity," *Earth Planet. Sci. Lett.*, vol.243, pp.149–158, 2006.
- [2] M. Kameyama, A. Kageyama, and T. Sato, "Multigrid iterative algorithm using pseudo-compressibility for three-dimensional mantle convection with strongly variable viscosity", *J. Comput. Phys.*, vol.206, no.1, pp.162–181, 2005.
- [3] M. Kameyama, "ACuTEMan: A multigrid-based mantle convection simulation code and its optimization to the Earth Simulator", *J. Earth Simulator*, vol.4, pp.2–10, 2005.
- [4] J. T. Ratcliff, G. Schubert, and A. Zebib, "Steady tetrahedral and cubic patterns of spherical shell convection with temperature-dependent viscosity," *J. Geophys. Res.*, vol.101, pp.25, 473–25, 484, 1996.
- [5] Y. Iwase, "Three-dimensional infinite Prandtl number convection in a spherical shell with temperature-dependent viscosity," *J. Geomag. Geoelectr.*, vol.48, pp.1499–1514, 1996.
- [6] T. Yanagisawa, and Y. Yamagishi, "Rayleigh-Benard convection in spherical shell with infinite Prandtl number at high Rayleigh number," *J. Earth Simulator*, vol.4, pp.11–17, 2005.

## マンテル対流と沈み込み過程の数値シミュレーション

プロジェクト責任者

深尾 良夫 海洋研究開発機構 地球内部変動研究センター

著者

深尾 良夫\*<sup>1</sup>, 亀山 真典\*<sup>2</sup>, 柳澤 孝寿\*<sup>1</sup>, 山岸 保子\*<sup>1</sup>, 中久喜伴益\*<sup>3</sup>

\*1 海洋研究開発機構 地球内部変動研究センター

\*2 愛媛大学 地球深部ダイナミクス研究センター

\*3 広島大学大学院 理学研究科

地球のマンテルを構成するのは岩石である。しかし地質学的な時間で見るとマンテルはゆっくりと流動していて、それが地表でのプレート運動を駆動して地震や火山という現象を引き起こし、更に長い時間スケールでは日本列島のような島弧やヒマラヤのような大山脈を作り出す原動力となる。よってマンテルの動きをモデル化することは地球の進化を考え、自然現象による我々の生存圏への影響を理解する上で極めて重要である。本プロジェクトでは、地球全体の進化過程を明らかにするために三次元球殻という形状の影響を考慮したマンテル全球対流モデルと、地震や火山現象の直接的原因であるプレートの地球内部への沈み込み過程を捉えるためにこの部分に特化した領域モデルの、双方の研究を行った。地震波トモグラフィーによると、沈み込んだプレートの延長と考えられる構造(スラブ)がマンテル遷移層の深さまで到達し、地球上の多くの場所ではそのまま遷移層に滞留している。これらはスタグナントスラブと呼ばれる。日本列島も含めた西太平洋域の地下にはスタグナントスラブが広域に存在し複雑な形態を示している。我々は前年度までに、二次元モデルによりスラブが滞留する条件を明らかにし、スラブの形状の時間発展をシミュレートすることに成功している。本年度からこれを三次元に拡張し、沈み込むプレートの年代が海溝軸に沿って異なるような状況も取り扱うことが可能となった。そして二次元の場合と同様に三次元でも下部マンテルでの粘性率の急激な増大がスタグナントスラブの形成に有効であることが示された。また海溝軸の後退の効果を取り入れた場合には、時間の経過とともにスラブの先端が大陸側へ入り込み、実際に西太平洋域で見られるような低角で傾斜した沈み込み形状をとることも示された。これらは沈み込みを対象とした領域モデルの結果であるが、一方で地球マンテルに対応する半径比を持つ3次元球殻内での熱対流のシミュレーションでも大きな進展が得られた。高解像度化と長時間積分により、マンテルのような高粘性流体の計算としては世界最高のレイリー数である $10^9$ に到達し、臨界値から6桁におよぶ対流のパターンと熱輸送に関する基礎的なデータセットを構築できた。各種統計量の解析から対流場の特徴がレイリー数にどのように依存するかというデータが得られ、これによりプレートなどの複雑性を考慮せずに全球を同時に扱うという観点では、地球史の大部分に適用できるレイリー数領域での熱対流の振舞いが明らかとなった。特に熱輸送量を表すヌセルト数が一貫してレイリー数の0.3乗程度で増大していくということが確立された。地球マンテルの進化は冷却に伴うレイリー数の低下として特徴づけられ、これらの結果は地球史の考察において不可欠な情報を与えるものである。

キーワード: マンテル対流, プレート沈み込み, 対流熱輸送